Microstructure and magnetic properties of sputtered Fe–Pt thin films

2003 J. Phys.: Condens. Matter 15 2561

(http://iopscience.iop.org/0953-8984/15/17/311)

INSTITUTE OF PHYSICS PUBLISHING JOURNAL OF PHYSICS: CONDENSED MATTER

J. Phys.: Condens. Matter **15** (2003) 2561–2571 PII: S0953-8984(03)57468-9

Microstructure and magnetic properties of sputtered Fe–Pt thin films

T Mahalingam[1,4], J P Chu[1,5], J H Chen[1], S F Wang[2] and K Inoue[3]

[1] Institute of Materials Engineering, National Taiwan Ocean University, Keelung 202, Taiwan, Republic of China
[2] Department of Materials and Mineral Resources Engineering, National Taipei University of Technology, Taipei 106, Taiwan, Republic of China
[3] Department of Materials Science and Engineering, University of Washington, Seattle, WA 98195-2120, USA

E-mail: jpchu@mail.ntou.edu.tw

Received 13 December 2002
Published 22 April 2003
Online at stacks.iop.org/JPhysCM/15/2561

Abstract

The characterization of rf magnetron-sputtered Fe–Pt thin films at various compositions (Pt = 15, 24, 46 and 78 at%) is reported. X-ray diffraction studies on annealed Fe–46%Pt thin films at 600 °C revealed an ordered $L1_0\gamma_2$-FePt phase with fct structure whereas annealed Fe–24%Pt and Fe–78%Pt films exhibited ordered γ_1-Fe_3Pt and γ_3-$FePt_3$ phases, respectively. The effects of argon quenching and rapid thermal annealing (RTA) on the structural and magnetic properties are investigated. When the films are annealed at 600 °C for 1 h and then quenched to room temperature in argon gas, ordered γ_2-FePt with $L1_0$ phase is obtained. Argon-quenched and rapid thermal annealed films exhibit microtwins in scanning electron microscopy analysis. The appearance of microtwins may be attributed to the planar defects developed in the FePt films due to the release of elastic strain during annealing. The saturation magnetization is found to increase with ferrous content in the films. Argon-quenched Fe–46%Pt films exhibited larger saturation magnetization than RTA-processed films. The large value of saturation magnetization obtained from M–H hysteresis indicates the predominant existence of the hard fct γ_2-FePt phase. The combined effects of twins, long-range order and the hard γ_2-FePt phase on the magnetic properties are discussed.

1. Introduction

In recent years, FePt binary alloy systems with the $L1_0\gamma_2$ phase have attracted much interest. The $L1_0$ phase consists of a monatomic, chemically modulated superlattice of the two

[4] Permanent address: Department of Physics, Alagappa University, Karaikudi 630 003, India.
[5] Author to whom any correspondence should be addressed.

elements [1]. The high magnetocrystalline anisotropy of FePt results in a high coercivity (H_c) and maximum energy product $(BH)_{max}$ which make this material a prime candidate for high-density magnetic recording applications. Epitaxially grown FePt thin films with their *c*-axis perpendicular to the film plane prepared by molecular beam epitaxy [2] and magnetron sputtering [3, 4] have been reported in the literature. Schwickert *et al* [5] have prepared a chemically ordered $L1_0$ phase of FePt using a temperature wedge method and correlated the magnetic properties with the chemical ordering of FePt films. The magnetic hardening in nanostructured Fe/Pt multilayer films prepared by a multiple-gun dc and rf sputtering system has been reported by Liu *et al* [6]. Kuo *et al* [7] reported the effect of W and Ti doping on the grain size and coercivity of Fe–50%Pt thin films. (Compositions in atomic per cent are used throughout this paper.) Tanaka *et al* [8] reported the observation of twins in FePt films and suggested that the high coercivity is attributed to the formation of antiphase boundaries. However, they reported that only poor magnetic properties are exhibited by the polytwin structures. Klemmer *et al* [9] attributed the enhanced coercivity of $L1_0$-type FePd films to the polytwin structure. Zhang and Soffa [10] reported that the hardness and magnetic properties of FePt alloys are improved due to the existence of twins in annealed samples. They found that the magnetic properties of FePt alloys strongly depend upon the sputtering conditions, alloy composition and post-deposition annealing treatment. Even though several reports are available in the literature regarding the preparation and characterization of FePt thin films, a systematic investigation on the effect of various annealing conditions on the microstructural and magnetic properties of FePt thin films is lacking. Hence, the present work deals with microstructural studies and evaluation of the magnetic properties of FePt alloy thin films and the effect of annealing conditions on the properties of magnetron-sputtered FePt thin films.

2. Experimental procedure

Fe–Pt alloy films of various compositions ($x = 15$, 24, 46 and 78 at%) were prepared by the rf magnetron sputtering technique onto silicon (100) substrates at room temperature. The deposition conditions usually affect the growth and properties of thin films. After several deposition runs, the following deposition parameters were fixed to prepare smooth and adherent FePt thin films: rf power 100 W, target to substrate distance 8 cm, working pressure 7×10^{-3} Torr. The silicon wafers were cleaned in a 5 vol% HF solution to remove native oxides and other contamination before loading into the sputtering chamber. A Pt target (99.9% pure) overlaid with an Fe plate (99.99% pure) was co-sputtered. Several overlying Fe target plates were fabricated so that the Pt target with different area fractions was exposed for co-sputtering and Fe–Pt films with various Fe contents were subsequently deposited. Fe–Pt thin films of thickness between 25 and 550 nm were sputter-deposited in a pure argon atmosphere at a working pressure of 7×10^{-3} Torr. Such deposited Fe–Pt alloy films were annealed in a vacuum of 10^{-7} Torr at various temperatures (400–800 °C) for 1 and 2 h. One group of films annealed at 600 °C was quenched in argon gas so as to cool them to room temperature in order to study the effect of quenching on their structural and magnetic properties. Another group of films was annealed in a rapid thermal annealing (RTA) furnace in an argon atmosphere at 400 and 600 °C. The samples were subjected to RTA for 10 s holding time. The heating and cooling rates for the RTA process were 10 and 40 °C s^{-1} respectively. The crystal structure and homogeneity of films were identified using a low glancing-angle thin-film x-ray diffractometer (XRD, Siemens D-5000) with Cu Kα radiation (K$\alpha = 1.5418$ Å). Field-emission scanning electron microscopy (SEM, Hitachi S4100) was used to analyse the microstructure of the films. The composition of the films was determined using an electron probe microanalyser (EPMA, JEOL JXA-8800M). The error of the standardless analysis was around $\pm 2\%$. The

compositional fluctuation at various points on the film surface was also determined and found to be very small (around 1%) which reveals the uniformity of the deposited films. The magnetic properties of the samples were measured with a vibrating sample magnetometer (VSM) (Micromag 2900). All the measurements (XRD, SEM and VSM) were carried out at room temperature.

3. Results and discussion

X-ray diffraction patterns of Fe–Pt films were recorded after annealing at 600 °C in a vacuum for 1 or 2 h. X-ray diffraction patterns of Fe–Pt films with three different Pt contents taken after annealing at 600 °C for 2 h are shown in figure 1. An x-ray diffraction pattern for as-deposited Fe–78%Pt film is also shown in the figure for comparison. XRD spectra of all the samples in the as-deposited condition reveal a γ phase with a prominent (111) peak at $\sim$40.5° of 2θ, as seen in figure 1(a). When the films are annealed at 600 °C for 1 h, on the other hand, Fe–78%Pt exhibits a $L1_2\gamma_3$-$FePt_3$ phase. For Fe–24%Pt, annealing under the same condition results in $L1_2\gamma_1$-Fe_3Pt as the major phase. In general, the peak broadening of Fe–Pt films becomes smaller in extent after annealing and the grain structure is expected to become coarse in annealed states. When films of Fe–78%Pt and Fe–24% Pt are annealed at 600 °C for 2 h, they maintain the same phases and the diffraction peak heights become sharper (figures 1(b) and (d)), as a result of the combined effects of grain growth, stress relaxation and improvement of crystallinity. On the other hand, when the film with composition Fe–46%Pt is annealed at 600 °C for 1 h, it revealed an ordered $L1_0\gamma_2$-FePt phase. It is also found that the superlattice reflections (001) and (110) begin to appear in the XRD spectra, indicating the formation of an ordered γ_2-FePt phase of Fe–46%Pt films. When the annealing duration is increased to 2 h, the heights of (001) and (110) peaks are found to increase, indicating an improvement in the crystallinity of the γ_2-FePt phase of the Fe–46%Pt film (figure 1(c)).

The typical XRD patterns of Fe–46%Pt films, 150 nm thick, argon quenched and RTA processed at 400 and 600 °C are shown in figure 2. As seen, the as-deposited Fe–46%Pt film shows broader peaks, indicating the nanocrystalline nature of the film. It is also found that the RTA-processed film at 400 °C exhibits only a disordered γ phase with fcc structure. It is noted that after annealing at 400 °C for 1 h an argon-quenched Fe–46%Pt film shows an ordered $L1_0\gamma_2$-FePt phase with fct structure. As seen in figure 2, the superlattice peaks (001) and (110) appear for the argon-quenched film after annealing at 400 °C for 1 h, indicating $L1_0$-type fct γ_2-FePt phase ordering. On the other hand, the RTA-processed film at 600 °C for 10 s shows the superlattice peaks (001) and (110), evidently indicating the presence of the ordered $L1_0\gamma_2$-FePt phase. When Fe–46%Pt films are annealed at 600 °C for 2 h and argon-quenched, it is observed that the disordered fcc (020) peak initially broadens and then splits into two peaks, which correspond to the (200) and (002) of the ordered fct γ_2-FePt phase. Similar behaviour was also observed in multilayered CoPt and FePt thin films, which was studied by Zeng *et al* [11]. It has been reported that ordering in bulk Fe–Pt specimens required annealing at elevated high temperatures for a couple of weeks and this long-term annealing was attributed to rather small interdiffusion coefficients of Fe and Pt atoms in the Fe–Pt alloy [12]. In the present work, however, the as-deposited Fe–Pt alloy thin films are in nanocrystalline form and the atomic ordering is thus achieved in a short time at 600 °C by rapid grain boundary motion, along with recrystallization which would be accompanied by enhanced intrinsic diffusion. Comparing the integrated intensity of the superlattice (200) and (020) reflections and the corresponding fundamental (111) reflections, the long-range atomic

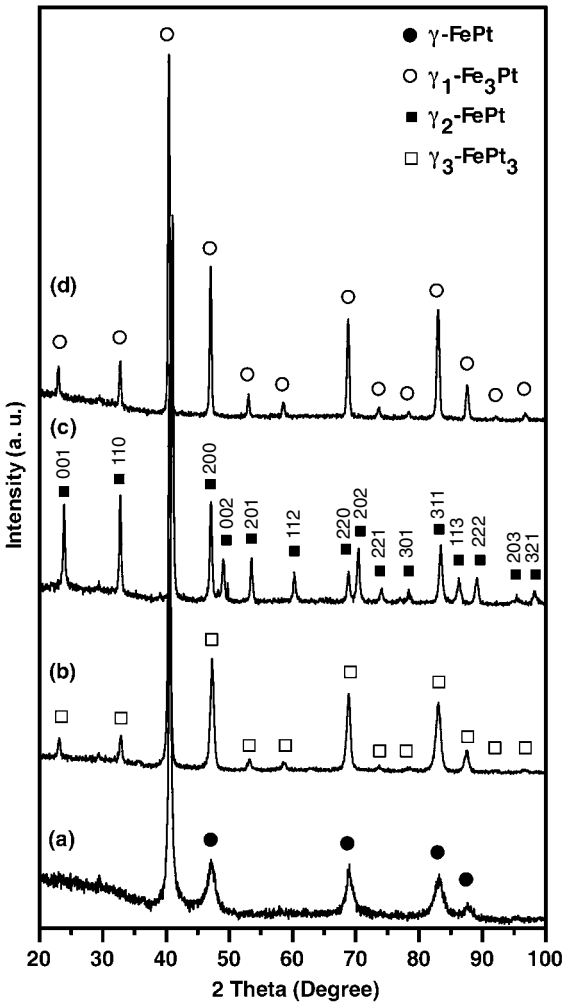

Figure 1. X-ray diffraction patterns of typical Fe–Pt thin films in as-deposited condition, Fe–78%Pt (a), and in as-annealed condition Fe–78%Pt (b), Fe–46%Pt (c) and Fe–24%Pt (d) at 600 °C for 2 h in vacuum.

ordering parameter K at a given temperature T may be obtained from the relation [13]

$$K = \frac{I_{S,T}/I_{(111),T}}{I_{S,600\,^\circ\mathrm{C}}/I_{(111),600\,^\circ\mathrm{C}}} \tag{1}$$

where the film annealed for 2 h at 600 °C is assumed to be perfectly ordered. Using the superlattice reflection lines (200) and (020), a long-range order parameter of $K = 0.90 \pm 0.05$ is estimated and this value is high and comparable with those reported earlier in other studies [1, 5].

To obtain high magnetic coercivity in Fe–Pt thin films, the films should also have a favourable microstructure. The plane views of scanning electron micrographs for Fe–46%Pt film annealed at 200, 400 and 800 °C are shown in figure 3. It is observed that as the annealing temperature is increased coalescence and aggregation of crystallites is evident, which is consistent with the XRD results described above. At an annealing temperature of 400 °C,

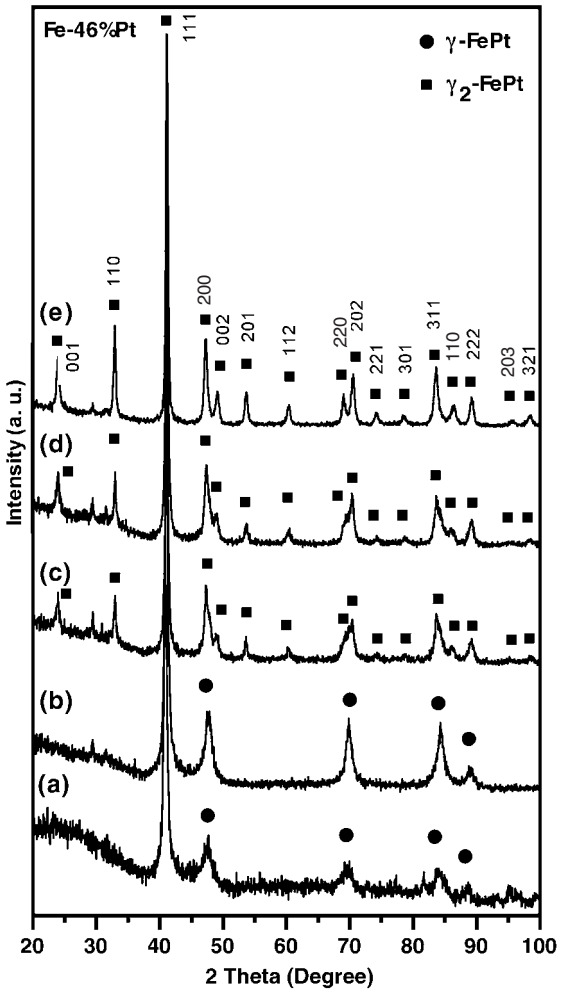

Figure 2. X-ray diffraction patterns of RTA-processed and argon-quenched Fe–46%Pt films for 1 h: (a) as-deposited, (b) RTA-processed and (c) argon-quenched at 400 °C, (d) RTA-processed and (e) argon-quenched at 600 °C.

aggregation of crystallites into larger grains takes place. When the films are annealed at 800 °C, the grains appeared in spherical shapes with average grain sizes in the range between 60 and 90 nm. The domain structure seems to be very sensitive to the size, shape and distribution of grains and hence this leads to the requirement for a favourable microstructure to obtain high coercivity in Fe–Pt thin films. Scanning electron micrographs of typical Fe–46%Pt films argon quenched and RTA processed at 400 and 600 °C are shown in figure 4. It is found that argon-quenched films at 400 °C (figure 4(a)) exhibit a smooth mosaic type structure with spherical grains. On the other hand, Fe–46%Pt films argon quenched at 600 °C exhibit lamellar-shaped microtwin structure, as seen in figure 4(b). It should be noted that RTA-processed films at 600 °C reveal a different type of microtwin with a needle-like structure as shown in figure 4(c). The occurrence of these microtwins in annealed films may be attributed to the planar defects, which may form in the $L1_0\gamma_2$-FePt thin films because of the contraction of the *c*-axis through a cubic-to-tetragonal transformation. During the structural transformation

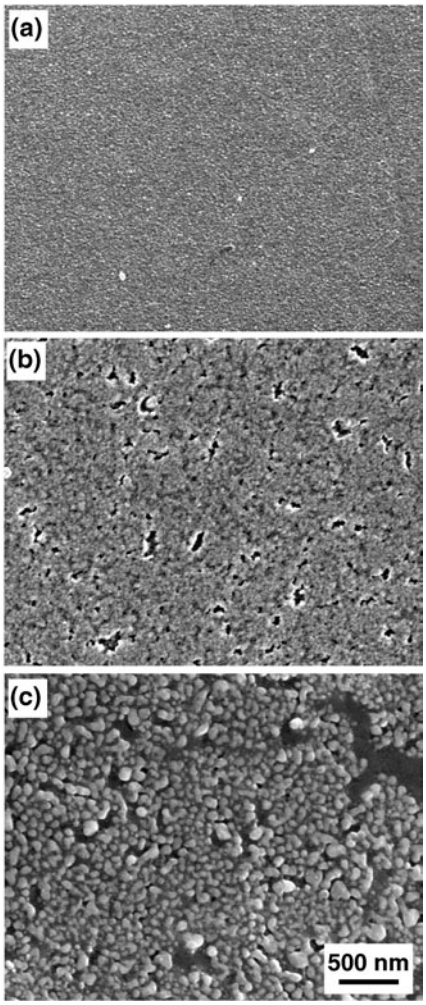

Figure 3. Plane-view scanning electron micrographs of Fe–46%Pt thin films vacuum annealed for 1 h at (a) 200 °C (b) 600 °C and (c) 800 °C.

into the $L1_0$ tetragonal phase, the microtwin structure is evolved to relieve the elastic strain associated with the $L1_0$ atomic ordering which may be regarded as 'transformation twins'. This observation is in accordance with the microtwin growth reported in bulk FePt alloys [12]. Moreover, twins formed in FePt alloy films are expected to reduce the medium noise [14].

The variations of saturation magnetization (M_s), the in-plane coercivity ($H_{c\parallel}$) and perpendicular coercivity ($H_{c\perp}$) for Fe–Pt films of thickness 175 nm are depicted in figure 5 as a function of ferrous content. As seen, the in-plane coercivity is greater than the perpendicular coercivity at lower ferrous content. The saturation magnetization is found to increase with ferrous content, becoming a maximum around 76 at% Fe, whereas the coercivity becomes a maximum at 50%Fe. The increase of M_s with decreasing Pt content may be attributed to the influence of Pt atoms in the Fe–Pt film lattice. It is worth mentioning that the best hard magnetic property of Fe–Pt alloy was reported near the stoichiometric composition (Fe–47.3%Pt) [15]. Watanabe [16] and Yung *et al* [17] have reported that the high coercively in FePt alloys is

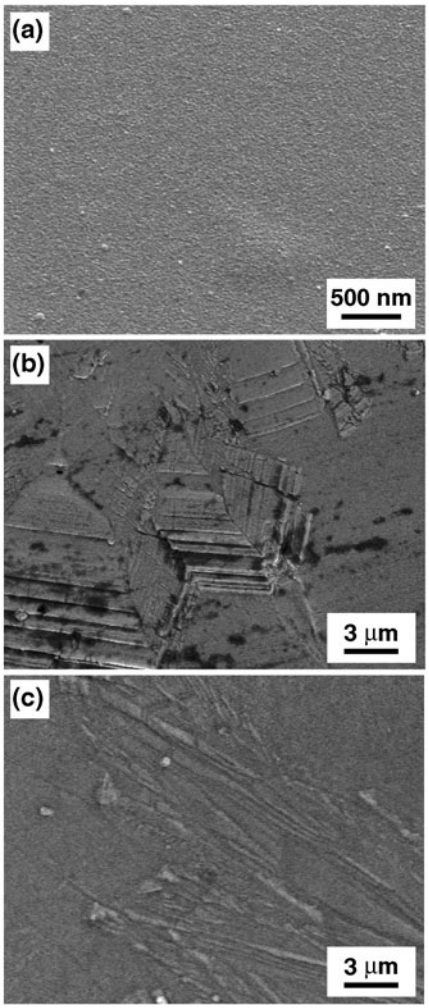

Figure 4. Scanning electron micrographs of typical Fe–46%Pt films: argon quenched at (a) 400 °C and (b) 600 °C, and (c) RTA processed at 600 °C.

related to the degree of imperfection in the fct γ_2-FePt phase. Kuo *et al* [18] have speculated that the critical diameter of the single-domain particle of the fct Fe–50%Pt phase may be about 90 nm to obtain high coercivity. They observed neither antiphase boundaries (APB) nor twins in their FePt films annealed at higher temperatures, which is in contradiction to the present study. As shown in figure 4, the present SEM study clearly showed that argon-quenched films at 600 °C with grain sizes of the order of 60–90 nm contained microtwins.

The variations of in-plane coercivity ($H_{c\|}$) for Fe–Pt films with four different compositions are shown in figure 6 as a function of annealing temperature. As seen, the coercivity is found to increase with annealing temperature for all Fe–Pt films studied and the increase is larger in Fe–46%Pt films, which are around 9.75 kOe. Further increase in annealing temperature is found to decrease the coercive field of the Fe–Pt films for all compositions. This may be attributed to a reaction between the Fe–Pt crystallites and the underlying silicon substrate. For the Fe–46%Pt films, the change of coercivity with annealing temperature may be attributed

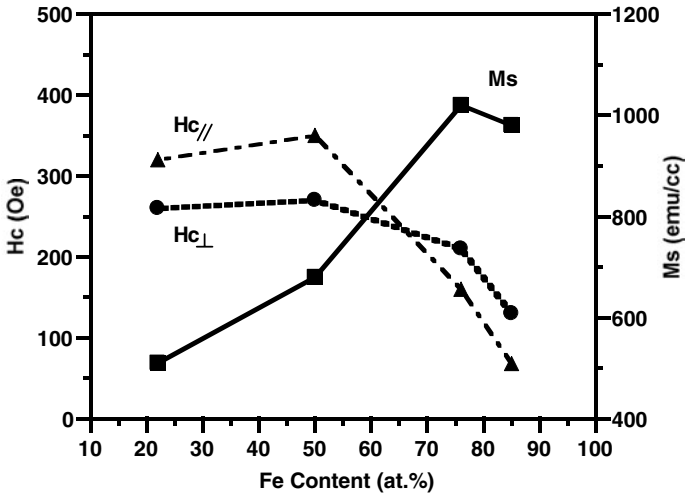

Figure 5. The variation of saturation magnetization (M_s) and coercivities ($H_{c\|}$ and $H_{c\perp}$) with ferrous content for Fe–Pt thin films.

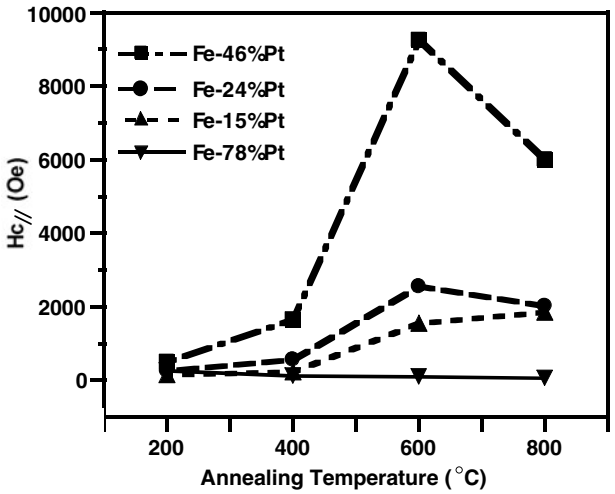

Figure 6. Variation of in-plane coercivity ($H_{c\|}$) with annealing temperature for various compositions of Fe–Pt films.

to the transformation of a disordered Fe_3Pt phase to an ordered γ_2-FePt phase, as shown in the present x-ray diffraction studies. At high annealing temperatures, the coercivity increases due to the improvement in crystallinity and the presence of twins. Consequently, the grain boundaries increase and they act as pinning sites for domain wall motion.

Figure 7 shows the variations in saturation magnetization (M_s) and squareness (S) of typical Fe–46%Pt films of thickness 175 nm with annealing temperature between 200 and 600 °C. As seen in this figure, the saturation magnetization M_s remains almost unchanged with annealing temperature up to 400 °C and then decreases rapidly up to an annealing temperature of 600 °C. A similar trend has already been reported for Fe–Pt based alloy thin films [18]. The saturation magnetization of Fe–Pt films annealed for a long time at high temperatures has

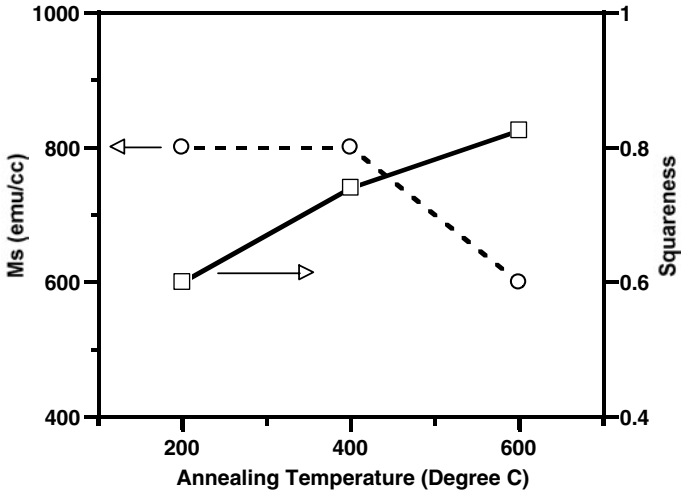

Figure 7. Variation of saturation magnetization (M_s) and squareness (S) of Fe–46%Pt film with annealing temperature.

a tendency to decrease due to the presence of very small grains of a phase with a low M_s that could reduce the saturation magnetization of the film as a whole [6]. A similar situation may cause a lower value of the saturation magnetization in our films in spite of the large value of coercivity observed in these films. The squareness, on the other hand, is found to increase from 0.60 to 0.80 between annealing temperatures of 200 and 600 °C. Further increase in annealing temperature to 800 °C resulted in a decrease in squareness, which may be caused by a reaction between the Fe–Pt film and the underlying silicon substrate.

It is known that the hysteresis behaviour of FePt alloy films depends strongly on the post-annealing treatments [18]. In order to examine the effect of annealing treatment and the successive cooling on the magnetic behaviour of Fe–46%Pt alloy films, $M-H$ loops are obtained using a VSM on argon-quenched and RTA-processed films after annealing at 600 °C. Some results obtained are depicted in figures 8(a) and (b), showing the VSM $M-H$ loops of a typical Fe–46%Pt film argon quenched at 600 °C for 1 h and RTA processed at 600 °C for 10 s respectively. As seen, $M-H$ loops exhibit a 'two-shoulder' behaviour for both cases, indicating an exchange coupling between magnetically soft fcc and hard fct phases. This may be due to the presence of a small amount of soft phase in the annealed Fe–Pt films. This further suggests a magnetic domain wall pinning motion mechanism as the dominant pinning mechanism in magnetron-sputtered FePt films. Similar behaviour was observed for Fe–Pt films prepared by sputtering Fe/Pt multilayers [19]. It is observed that the argon-quenched film exhibited larger values of M_s than RTA-processed film at 600 °C.The enormous change in the magnetization values between argon-quenched and RTA-processed films at 600 °C may be attributed to the difference in magnetic hardness achieved by the films during the annealing process. It appears that argon-quenched films acquired higher magnetic hardness than the RTA-processed films in our present studies. This is also evidenced by the higher long-range order parameter estimated for the argon-quenched films than RTA-processed films. The shorter RTA time (10 s) may be the main reason for the poor performance of RTA-processed films in achieving higher long-range ordering and magnetic hardness in FePt films. The planar defects in the Fe–46%Pt films which appear as microtwins may be acting as pinning centres for domain wall motion in argon-quenched film. This, in turn, may cause an exchange coupling between

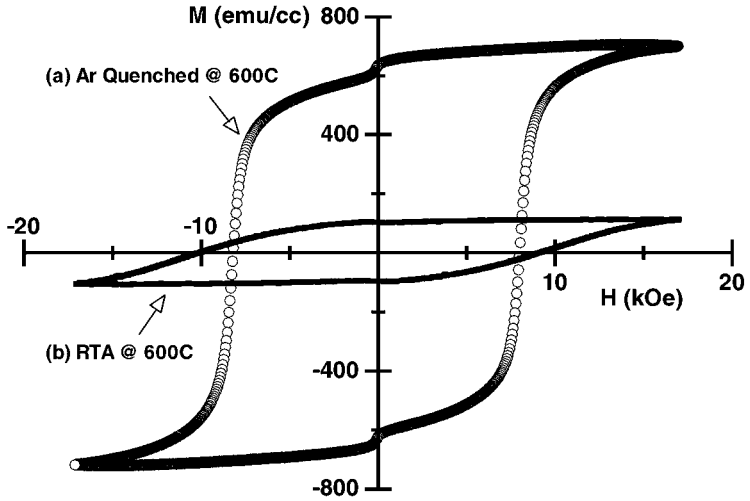

Figure 8. M–H loops of typical Fe–46%Pt films (a) annealed at 600 °C for 1 h and argon quenched and (b) RTA processed at 600 °C for 10 s.

the magnetically hard fct γ_2-FePt phase and the soft fcc γ-FePt phases. It may be concluded that the microtwinned structure observed in the present study could be favourable for Fe–Pt films having a magnetically hard fct γ_2-FePt phase to improve magnetic properties. In this regard, Zhang *et al* [20] reported that instead of microtwins the APB in the microtwinned structure plays a vital role in achieving magnetic hardness in FePt permanent magnets.

An energy product $(BH)_{\max}$ of about 13 MG Oe is obtained for 600 °C annealed and argon quenched Fe–46%Pt films. This magnetic property is comparable to that reported by Kuo *et al* [18], who studied Fe–50%Pt films annealed at 600 °C for 30 min followed by furnace cooling. Because of such a high magnetic energy, the magnetic property of the present Fe–Pt films annealed at 600 °C and argon quenched is considered to be suitable for magnetic film applications.

4. Conclusions

Fe–Pt alloy thin films with various compositions were prepared by an rf magnetron sputtering method. X-ray diffraction studies on rf-sputtered Fe–46%Pt films annealed at 600 °C for 1 h and argon quenched exhibited ordered γ_2-FePt ($L1_0$) phase with an fct structure. A long-range atomic ordering parameter of 0.90 indicates the high ordering of Fe–46%Pt films treated by argon quenching at 600 °C. The appearance of microtwins as observed in SEM on annealed films may be attributed to the planar defects in the Fe–46%Pt films, indicating the release of interfacial stress by a cubic to tetragonal transformation. The saturation magnetization is found to increase with ferrous content in the Fe–Pt alloy films. The large values of M_s and $H_{c\|}$ for Fe–46%Pt may be attributed to the existence of a pure γ_2-FePt phase in the film. It is observed that argon-quenched films exhibited larger saturation magnetization than RTA-processed films. Magnetic hysteresis studies indicate that a magnetic domain wall pinning motion mechanism is the dominant pinning mechanism in FePt films. The coercivity and the energy product $(BH)_{\max}$ obtained for argon-quenched films at 600 °C are high (9.75 kOe and 13 MG Oe, respectively), suggesting that the rf magnetron-sputtered FePt films may be useful for magnetic film applications.

Acknowledgments

One of the authors (JPC) would like to thank Professor T S Chin of National Lien-Ho Institute of Technology and Professor P C Kuo of National Taiwan University for their valuable comments and encouragements. This work is supported by National Science Council of the Republic of China (NSC-90-2216-E-019-003 and NSC-91-2811-E-019-001), which is gratefully appreciated.

References

[1] Thiele J-U, Folks L, Toney M F and Weller D K 1998 *J. Appl. Phys.* **84** 5686
[2] Cebollada A, Weller D, Sticht J, Harp G H, Farrow R F C, Marks R F, Savoy R and Scott J C 1994 *Phys. Rev.* B **50** 3419
[3] Watanabe M and Homma M 1996 *Japan. J. Appl. Phys.* 1 **35** 1264
[4] Kuo C M, Kuo P C, Wu H C, Yao Y D and Lin C H 1999 *J. Appl. Phys.* **85** 4886
[5] Schwickert M M, Hannibal K A, Toney M F, Best M, Folks L, Thiele J U, Kellock A J and Weller D 2000 *J. Appl. Phys.* **87** 6956
[6] Liu J P, Liu Y, Luo C P, Shan Z S and Sellmyer D J 1997 *J. Appl. Phys.* **81** 5644
[7] Kuo C M, Kuo P C, Hsu W C, Li C T and Sun A C 2000 *J. Magn. Magn. Mater.* **209** 100
[8] Tanaka Y, Kimura N, Hono K, Yasuda K and Sakurai T 1997 *J. Magn. Magn. Mater.* **170** 289
[9] Klemmer T, Hoydick D, Okumura H, Zhang B and Soffa W A 1995 *Scr. Metall.* **33** 1793
[10] Zhang B and Soffa W A 1992 *Phys. Status Solidi* a **131** 707
[11] Zeng H, Yan M L, Powers N and Sellmyer D J 2002 *Appl. Phys. Lett.* **80** 2350
[12] Mrowec S 1980 *Material Science Monographs* vol 5 (Amsterdam: Elsevier)
[13] Wang S H, Feng Q and Gao Y Q 1998 *Acta Mater.* **46** 6485
[14] Suzuki T, Kiya T, Honda N and Ouchi K 2001 *J. Magn. Magn. Mater.* **235** 312
[15] Hong M H, Hono K and Watanabe M 1998 *J. Appl. Phys.* **84** 4403
[16] Watanabe K 1988 *Mater. Trans. JIM* **29** 80
[17] Yung S W, Chang Y H, Lin T J and Hung M P 1992 *J. Magn. Magn. Mater.* **116** 411
[18] Kuo C M, Kuo P C and Wu H C 1999 *J. Appl. Phys.* **85** 2264
[19] Liu J P, Luo C P, Liu Y and Sellmyer D J 1998 *Appl. Phys. Lett.* **72** 483
[20] Zhang B, Lelovic M and Soffa W A 1991 *Scr. Metall.* **25** 1577